韓藥作誌(Korean J. Medicinal Crop Sci.) 34(5) : 293 – 311 (2026)
ISSN(Print) 1225-9306
ISSN(Online) 2288-0186
http://www.medicinalcrop.org
http://dx.doi.org/10.7783/KJMCS.2026.34.5.293

볶은 대추야자(*Phoenix dactylifera*) 씨앗의 열수 추출물에 대한 파이토케미컬 특성 분석, α-아밀라아제 결합 분자 도킹 및 급성 독성 평가

은조쿠 아쿠도 제너비브[1] · 은조쿠헨리 도리스 오비아게리[2] · 추쿠마 라파엘 에케아냔우[3†]

Phytochemical Characterisation, α-Amylase-Binding Molecular Docking, and Acute Toxicity Assessment of Hot Aqueous Extract from Roasted *Phoenix dactylifera* Seeds

Njoku Akudo Genevieve[1], Njoku-Henry Doris Obiageri[2], and Chukwuma Raphael Ekeanyanwu[3†]

Received: 2026 August 09
1st Revised: 2026 August 28
2nd Revised: 2026 September 24
3rd Revised: 2026 October 02
Accepted: 2026 October 02
Published: 2026 October 30

This is an open access article distributed under the terms of the Creative Commons Attribution Non-Commercial License (http://creativecommons.org/licenses/by-nc/3.0/) which permits unrestricted non-commercial use, distribution, and reproduction in any medium, provided the original work is properly cited.

ABSTRACT

Background: Globally, > 537 million adults have type 2 diabetes mellitus, and its prevalence is increasing in Nigeria due to urbanization and changes in diet. Standard treatments have downsides such as side effects and cost. Date palm (*Phoenix dactylifera*) seeds, an agro-waste traditionally used for metabolic disorders, have potential.

Methods and Results: Fourier transform-infrared spectroscopy (FT-IR) and gas chromatography–mass spectrometry (GC–MS) were used to characterize the roasted date seeds hot aqueous infusion (HAERD) and its ability to inhibit α-amylase was predicted by molecular docking and acute oral toxicity (OECD 423) was evaluated. FT-IR spectral features were tentatively consistent with carbohydrate and phenolic/aromatic-type functional groups although phenolic content was not quantitatively determined. GC–MS revealed that methyl oleate (27.77%) was the major constituent followed by methyl ricinoleate (12.76%), methyl linoleate (7.58%), and cis-vaccenic acid (8.41%). Docking to human pancreatic α-amylase (PDB: 1B2Y) revealed binding affinities of −4.6 to −6.2 ㎉/㏖ for the seven ligands from extracts, with methyl oleate displaying the highest affinity among the seven ligands (−6.2 ㎉/㏖, hydrogen bond with Thr6). Acarbose (positive control) showed higher binding affinities than the seven ligands (−7.4 ㎉/㏖). None of the eight ligands, including acarbose, interacted with the canonical catalytic triad (Asp197, Glu233, and Asp300). No mortality or clinical toxicity was observed up to 5000 ㎎/㎏ (LD_{50} > 5000 ㎎/㎏; GHS Category 5, low acute lethality classification, not absence of toxicity) but histopathological assessment showed dose-dependent hepatic, renal, and cardiac changes that were pronounced at the limit dose (5000 ㎎/㎏), including hepatocellular disorganization, renal tubular degeneration, and myocardial fiber disruption.

Conclusions: HAERD has a good acute safety profile and potential α-amylase inhibitory activity from in silico docking, indicating future research for its traditional use and development into a sustainable nutraceutical from agro-waste.

Key Words: *Phoenix dactylifera*, Date Palm Seeds, Hot Water Infusion, Phytochemical Characterization, Molecular Docking, Pancreatic α-amylase, Acute Oral Toxicity

INTRODUCTION

Type 2 diabetes mellitus is one of the most pressing public health challenges worldwide. Based on the 11th edition of the International Diabetes Federation (IDF) Diabetes Atlas (Genitsaridi *et al*., 2026), the prevalence of diabetes was 589 million adults in 2024, and it is expected to reach 853 million by 2050. The burden is especially high in low- and middle-income countries, accounting for about four in five (81%) of all cases. In Nigeria, prevalence has increased over recent decades due to

†Corresponding author: (Phone) +234-806-095-5950 (E-mail) ekeanyanwu.chukwuma@imsuonline.edu.ng
[1]이모 주립대학교 생화학과 연구원 / Researcher, Department of Biochemistry, Imo State University, P.M.B. 2000, Owerri, Imo State, Nigeria
[2]이모 주립대학교 생화학과 연구원 / Researcher, Department of Biochemistry, Imo State University, P.M.B. 2000, Owerri, Imo State, Nigeria
[3]이모 주립대학교 생화학과 부교수 / Associate Professor, Department of Biochemistry, Imo State University, P.M.B. 2000, Owerri, Imo State, Nigeria

rapid urbanisation, dietary changes toward high carbohydrate diets and sedentary lifestyles. Nigeria has an estimated 3.0 million adults with diabetes, the highest burden in the IDF Africa Region, with an age-standardised prevalence of 3.0%, projected to increase to 6.6 million by 2050 (IDF, 2025), more than doubling the current figure. Conventional antidiabetic agents remain the cornerstone of therapy but have notable limitations. Metformin, the first-line drug, primarily acts by suppressing hepatic gluconeogenesis and improving peripheral insulin sensitivity through activation of AMP-activated protein kinase (AMPK). Sulfonylureas stimulate insulin secretion from pancreatic β-cells by closing ATP-sensitive potassium channels, leading to membrane depolarisation and calcium influx. Insulin therapy directly replaces or supplements endogenous insulin to promote glucose uptake and inhibit hepatic glucose production. While effective, these agents are frequently associated with adverse effects including gastrointestinal intolerance (metformin), hypoglycaemia and weight gain (sulfonylureas and insulin), and high treatment costs, which compromise long-term adherence, especially in resource-limited settings (Maruthur *et al*., 2016).

These challenges have intensified scientific interest in natural products from traditionally used medicinal plants, particularly those derived from underutilised agro-industrial waste. The seeds of the date palm (*Phoenix dactylifera* L.), which constitute 10–15% of the fruit and are frequently discarded as agro-waste, have a long history of use in Middle Eastern and North African ethnomedicine for the management of diabetes and metabolic disorders (Vayalil, 2012; Djaoudene *et al*., 2026). Recent research has highlighted the rich phytochemical profile of date palm seeds, including polysaccharides, phenolic acids, flavonoids, and unsaturated fatty acid esters (Alkhoori *et al*., 2022; Alfaleh and Sindi, 2024). Several studies have reported hypoglycaemic, hypolipidaemic, and antioxidant activities of date seed extracts in streptozotocin- or high-fat diet-induced diabetic models (Hasan and Mohieldein, 2016; Khan *et al*., 2018; Alqarni *et al*., 2019).

Similar investigations on Nigerian medicinal plants such as *Vernonia amygdalina* and *Gongronema latifolium* have demonstrated significant antihyperglycaemic and antioxidant effects in high-carbohydrate diet models (Ugochukwu *et al*., 2003; Egedigwe *et al*., 2016). However, comprehensive studies that combine detailed phytochemical characterisation, molecular docking against key carbohydrate-metabolising enzymes such as human pancreatic α-amylase, and rigorous acute toxicity assessment of the traditionally prepared hot water infusion from roasted date palm seeds remain limited.

The present study therefore aimed to characterise the phytochemical profile of the hot water infusion of roasted *Phoenix dactylifera* seeds (HAERD) using FT-IR and GC–MS, evaluate the binding affinities of its major constituents to human pancreatic α-amylase through molecular docking, and assess its acute oral toxicity according to OECD Guideline 423 (OECD, 2002). By integrating ethnomedicinal knowledge with contemporary analytical and computational methods, this work seeks to provide a scientific foundation for the traditional use of roasted date palm seed infusion and to explore its potential as a sustainable, accessible nutraceutical derived from agricultural waste.

MATERIALS AND METHODS

1. Equipment

All experimental procedures, including sample preparation, phytochemical characterisation, and acute toxicity assessment, were performed using standard laboratory equipment available at the Department of Biochemistry Laboratory, Imo State University, Owerri, Nigeria, and the Multi-User Science Laboratory, Ahmadu Bello University, Zaria, Nigeria. The major equipment included a Memmert oven, Model UN30 (Memmert GmbH + Co. KG, Schwabach, Germany); Kartell desiccator, Model 550 (Kartell S.p.A., Noviglio, Italy); Kenwood electric grinder, Model BL335 (Kenwood Limited, Havant, UK); Endecotts stainless-steel test sieve, 1.00 mm aperture, 203.2 mm diameter, ASTM E11 (Endecotts Ltd., London, UK); Sigma-Aldrich airtight amber-coloured glass bottles (Sigma-Aldrich Co., St. Louis, MO, USA); Haier Biomedical laboratory refrigerator, Model HLR-310F, 310 L (Haier Biomedical, Qingdao, China); Büchi Rotavapor R-100 rotary evaporator (Büchi Labortechnik AG, Flawil, Switzerland); Labconco FreeZone 4.5 L benchtop freeze dryer (Labconco Corporation, Kansas City, MO, USA); Agilent 7890B gas chromatograph coupled to an Agilent 5977A series mass selective detector (MSD) equipped with an electron ionization (EI) source, fitted with an HP-5MS capillary column (Agilent Technologies, Santa Clara, CA, USA); Agilent Cary 630 FT-IR spectrometer (Agilent Technologies, Santa Clara, CA, USA); Eppendorf Centrifuge 5430R refrigerated centrifuge (Eppendorf SE, Hamburg, Germany); Thermo Scientific GENESYS 50 UV-Vis spectrophotometer (Thermo Fisher Scientific, Waltham, MA, USA); Thermo Scientific TSX 60086A ultra-low

temperature (−80℃) freezer (Thermo Fisher Scientific, Waltham, MA, USA); Leica RM2125 RTS manual rotary microtome (Leica Biosystems, Wetzlar, Germany); Olympus BX43 upright microscope with digital photomicrographic system (Olympus Corporation, Tokyo, Japan); a laboratory-grade liquid nitrogen storage container (cryogenic dewar vessel); and Whatman No. 1 filter paper (Cytiva, Marlborough, MA, USA).

2. Reagents and chemicals

All reagents and chemicals were procured from verified reputable suppliers and used strictly according to the manufacturers' instructions and within their specified expiry periods to ensure accuracy and reproducibility of results. The major reagents and chemicals included analytical-grade methanol, ethanol, sulphuric acid, trichloroacetic acid, and n-butanol from Merck (Germany), 10% neutral-buffered formalin and phosphate-buffered saline from Merck (Germany), and spectroscopic-grade potassium bromide (KBr) for FT-IR analysis.

3. Plant material

Dry fruits of *Phoenix dactylifera* (date palm) were purchased from a reputable local market in Kano State, Nigeria. The seeds were manually separated from the fruit pulp, thoroughly washed with distilled water to remove any adhering fruit residues, and air-dried at room temperature. Botanical identification and authentication were carried out by Dr C.I.N Unamba, a plant taxonomist at the Department of Plant Science and Biotechnology (Botany), Imo State University, Owerri, Nigeria. A voucher specimen (Voucher No.: IMSU/PSB/PHOENIX/024) was deposited in the university herbarium for future reference.

4. Experimental animals

Healthy adult male Wistar albino rats (*Rattus norvegicus*) weighing between 95–195 g were used for this study. The animals were procured from the Animal House Unit, Department of Anatomy, Imo State University, Owerri, Nigeria. Upon arrival, the animals were housed in clean, well-ventilated standard plastic cages with stainless steel wire lids and wood shavings as bedding. The rats were maintained under controlled environmental conditions:

Temperature: 22 ± 2℃
Relative humidity: 55 ± 10%
Light/dark cycle: 12 hours light and 12 hours dark

The animals were allowed two weeks of acclimatisation to laboratory conditions before the commencement of the experiment. During this period, they were fed standard rat chow (Vital Feed, Nigeria) and had free access to clean drinking water ad libitum.

5. Ethical approval

The experimental protocol for the acute oral toxicity study was reviewed and approved by the Institutional Animal Care and Use Committee (IACUC) of Imo State University, Owerri, Nigeria (Approval No. 13706; approved 8 November 2025), prior to commencement. All procedures were conducted in strict accordance with the Guide for the Care and Use of Laboratory Animals (NRC, 2011) and the ARRIVE 2.0 guidelines for reporting animal research (Percie du Sert *et al*., 2020). Humane endpoints were clearly defined and included sustained body weight loss of ≥ 20% within 7 days, severe lethargy, persistent severe diarrhoea, impaired mobility, or any signs of acute distress. Animals reaching these endpoints were immediately humanely euthanised under ketamine/xylazine anaesthesia to minimise suffering. Personnel involved in clinical observations and histopathological evaluations were blinded to treatment allocation wherever feasible to reduce observer bias. The number of animals used (n = 3 per group) was minimised in accordance with OECD Guideline 423 while ensuring sufficient statistical power for safety assessment.

6. Preparation of hot water extract of roasted date seeds

The seeds were manually separated from the fruit pulp, thoroughly washed with distilled water to remove residual sugars and organic matter, and air-dried under shade at ambient temperature (25–28℃) for 10–14 days to ensure complete moisture removal (Al-Farsi and Lee, 2008b). The dried seeds were then roasted at 180℃ for 15 minutes in a controlled oven to enhance flavour and bioactivity through the formation of Maillard reaction products, while minimising the degradation of thermolabile compounds such as flavonoids (Al Juhaimi *et al*., 2018; Ismail *et al*., 2025). After roasting, the seeds were cooled to room temperature, milled into a fine powder using a laboratory mechanical grinder, and sieved to obtain a uniform particle size, ensuring consistency in the extraction process.

The hot water extract was prepared using a modified traditional decoction method aimed at preserving thermolabile and water-soluble bioactive constituents, such as phenolic acids and polysaccharides, whose bioavailability is enhanced by roasting

(Li *et al*., 2023; Swaidan *et al*., 2023). Specifically, 100 g of roasted seed powder was added to 1 litre of boiling distilled water and maintained at a gentle boil for 60 minutes with intermittent stirring to optimise the extraction of bioactive compounds. The mixture was then cooled to room temperature and filtered using Whatman No. 1 filter paper. The filtrate was concentrated under reduced pressure at 40℃ using a rotary evaporator and subsequently lyophilised to obtain a stable dry powder. The dried extract was stored in amber-coloured, airtight containers at 4℃ to prevent phenolic compound degradation, thereby ensuring stability for subsequent phytochemical and pharmacological analyses.

7. Gas chromatography–mass spectrometry (GC–MS)

Gas chromatography–mass spectrometry (GC–MS) analysis was performed to identify and semi-quantify volatile and semi-volatile compounds in the lyophilised hot aqueous extract. Approximately 10 mg of the lyophilised extract was dissolved in 1 mL of analytical-grade methanol (10 mg/mL), vortex-mixed, and filtered through a 0.22 µm syringe filter. A 1 µL aliquot was injected in splitless mode into an Agilent 7890B gas chromatograph coupled to a 5977A mass selective detector, equipped with an HP-5MS capillary column (30 m × 0.25 mm i.d., 0.25 µm film thickness). The oven temperature program was set as follows: initial hold at 50℃ for 2 min, increased at 10℃/min to 300℃, and held for 5 min. Helium was used as the carrier gas at a constant flow rate of 1.2 mL/min. The mass spectrometer operated in electron ionisation (EI) mode at 70 eV. Compounds were identified by comparison of their mass spectra with the NIST/EPA/NIH Mass Spectral Library (NIST 14) (NIST, 2014), with match factors > 70% considered acceptable. System suitability was confirmed using blank injections and an n-alkane standard mixture (C8–C40). Semi-quantification was based on relative peak area percentages.

8. Fourier-transform infrared spectroscopy (FT-IR)

Fourier-transform infrared (FT-IR) spectroscopy was used to characterise the major functional groups in the lyophilised hot aqueous extract. Approximately 2 mg of the dry extract was homogenised with 100 mg of spectroscopic-grade potassium bromide (KBr) in an agate mortar. The mixture was compressed under 8 tons of pressure for 1 min to form a translucent pellet (~1 mm thick). Spectra were recorded in transmission mode on an Agilent Cary 630 spectrometer over the range 4000–400 cm^{-1} at a resolution of 4 cm^{-1} with 32 co-added scans. A background spectrum of a blank KBr pellet was subtracted. Absorption bands were assigned using standard correlation tables and literature spectra of date palm seed extracts (Silverstein *et al*., 2015).

9. Molecular docking against human pancreatic α-amylas

Molecular docking studies were conducted using AutoDock Vina 4.2.6 and AutoDockTools 1.5.7 (Morris *et al*., 2009) to evaluate the binding affinities and molecular interactions of major phytoconstituents identified by GC–MS with human pancreatic α-amylase (EC 3.2.1.1), a key enzyme in starch digestion and a validated target for postprandial hyperglycaemia control. Seven major compounds identified by GC–MS — methyl ricinoleate (12.76%), methyl oleate (27.76%), oleic acid (0.38%), methyl linoleate (7.58%), cis-vaccenic acid (8.41%), methyl 14-methylpentadecanoate (1.13%), and squalene (1.37%) — were selected as ligands on the basis of their reported relevance as α-amylase-interacting constituents in the phyto-chemical and enzyme-inhibition literature, rather than GC–MS abundance alone; consequently, some abundant constituents without established relevance to carbohydrate-digesting enzyme interactions (e.g., methyl stearate, 4.41%) were not included, while lower-abundance constituents with documented relevance (e.g., oleic acid, 0.38%) were retained, with acarbose used as the positive control. Three-dimensional structures of the ligands were retrieved from PubChem or constructed in ChemDraw Professional 20.0 and energy-minimised using the MMFF94 force field in Avogadro 1.2.0. The X-ray crystal structure of human pancreatic α-amylase in complex with acarbose (PDB ID: 1B2Y; resolution 3.2 Å) was obtained from the Protein Data Bank (Berman *et al*., 2000). Although higher-resolution structures of human pancreatic α-amylase are available in the Protein Data Bank — notably the apo structure 1B2Y, resolved at 1.8 Å (Brayer *et al*., 1995) — the acarbose-bound holo structure 1B2Y was selected in preference to these because it captures the enzyme in complex with acarbose (Nahoum *et al*., 2000), the same compound used as the positive control in this study. This choice enabled direct validation of the docking protocol by redocking acarbose into its native, crystallographically resolved pose, a validation step that an apo structure lacking a bound reference ligand cannot provide. The catalytic residues (Asp197, Glu233, Asp300) and overall active-site architecture are conserved between the 1.8 Å apo form and the 3.2 Å acarbose-bound form, so the modest reduction in resolution was judged an acceptable trade-off for the gain in docking-

protocol validation confidence. Water molecules and the co-crystallised ligand were removed, polar hydrogens added, and Gasteiger charges assigned using AutoDockTools 1.5.7. A grid box of 40 × 40 × 40 points with 0.375 Å spacing was centred at coordinates x = 17.982, y = 21.308, z = 49.35 to encompass the catalytic domain. Docking was performed using the Lamarckian Genetic Algorithm with 100 independent runs, a population size of 150, and a maximum of 2,500,000 energy evaluations per run. The lowest-energy binding pose was selected for each ligand. The docking protocol was validated by redocking acarbose, which reproduced the crystallographic pose with an RMSD of 0.000 Å. Binding free energies (㎉/㏖) and protein–ligand interactions were analysed and visualised using BIOVIA Discovery Studio Visualizer 2021 and PyMOL 2.5.

10. ADME/Tox prediction

In silico absorption, distribution, metabolism, and excretion (ADME) and toxicity properties of the seven major GC–MS-identified constituents used in molecular docking, together with acarbose as reference, were predicted using SwissADME (Daina *et al*., 2017) and pkCSM (Pires *et al*., 2015). Canonical SMILES for each compound were retrieved from PubChem and submitted to both web servers using default parameters. Parameters evaluated included compliance with Lipinski's rule of five (SwissADME), gastrointestinal (GI) absorption and blood–brain barrier (BBB) permeability (pkCSM), cytochrome P450 (CYP450) isoform inhibition (SwissADME), predicted hepatotoxicity and AMES mutagenicity (pkCSM), and predicted oral toxicity (rat LD_{50}, pkCSM).

11. Acute toxicity study

The acute oral toxicity of the lyophilised hot aqueous extract was evaluated in accordance with OECD Test Guideline 423 (OECD, 2002), an acute toxic class procedure that enables classification of substances under the Globally Harmonised System (GHS) while minimising animal use through a stepwise limit-test design and small group sizes. Animals were randomly assigned to three groups: vehicle control (distilled water), 2000 ㎎/㎏ body weight, and 5000 ㎎/㎏ body weight of the hot aqueous extract. These doses represent the limit doses specified in OECD Guideline 423, allowing determination of whether the median lethal dose (LD_{50}) exceeds 2000 ㎎/㎏ or 5000 ㎎/㎏, or identification of higher toxicity categories if mortality or severe clinical signs are observed. The lyophilised extract was reconstituted in distilled water immediately prior to administration to ensure homogeneity and stability. Rats were fasted overnight (approximately 12–16 h, water freely available) to standardise gastrointestinal conditions and improve absorption consistency. Dosing was performed as a single oral gavage using appropriately sized stainless steel gavage needles and syringes, with the maximum dosing volume not exceeding 20 mL/kg body weight. Post-dosing observations commenced immediately and continued continuously for the first 4 hours to detect acute toxic signs (e.g., mortality, convulsions, tremors, salivation, lacrimation, piloerection, diarrhoea, dyspnoea, cyanosis, altered gait, abnormal posture, or changes in respiration, skin, fur, or mucous membranes). Thereafter, animals were subjected to at least once-daily detailed clinical observations throughout the 14-day observation period. Body weight was recorded on Days 0 (pre-dosing), 7, and 14 to monitor potential treatment-related effects on growth, food and water intake, or overall health status. At the end of the 14-day observation period, all surviving animals were humanely euthanised under deep anaesthesia (ketamine/xylazine combination). Gross necropsy was performed to examine major organs (liver, kidneys, and heart) for macroscopic abnormalities such as discolouration, enlargement, haemorrhage, congestion, or gross lesions. The liver, kidneys and heart were harvested, fixed in 10% neutral-buffered formalin for at least 24 hours, processed through routine histological techniques (graded ethanol dehydration, xylene clearing, paraffin embedding), sectioned at 4–5 ㎛ thickness, and stained with haematoxylin and eosin (H&E) for microscopic evaluation of potential target organ toxicity or histopathological alterations (Bancroft and Gamble, 2019).

12. Sample collection

Tissue sampling was conducted using humane and standardised procedures to obtain high-quality specimens for histopathological evaluation while prioritising animal welfare and minimising distress. All procedures were performed by trained personnel in strict accordance with the approved Institutional Animal Care and Use Committee (IACUC) protocol of Imo State University Owerri (Approval No. 13706; approved 8 November 2025), the National Research Council's *Guide for the Care and Use of Laboratory Animals* (NRC, 2011), and the ARRIVE 2.0 guidelines (Percie du Sert *et al*., 2020). At the end of the 14-day observation period, surviving rats were deeply anaesthetised with a ketamine/xylazine combination administered intraperitoneally and humanely euthanised. Immediately after confirmation of death, a midline abdominal

incision was made, and the liver, kidneys, and heart were carefully excised. Organs were rinsed briefly in ice-cold physiological saline (0.9% NaCl), blotted dry on sterile filter paper, and weighed to determine absolute and relative organ weights. Representative sections (approximately 1 cm^3) from each organ were fixed in 10% neutral-buffered formalin (fixative volume at least 10 times the tissue volume) for 48 h. Fixed tissues were labelled with animal identification number, group, organ, and fixation date, then processed using standard histological techniques (graded ethanol dehydration, xylene clearing, paraffin embedding). Sections were cut at 5 μm thickness using a rotary microtome and stained with haematoxylin and eosin (H&E) for microscopic evaluation by a histopathologist blinded to treatment allocation (Bancroft and Gamble, 2019). Evaluations focused on tissue architecture, cellular morphology, necrosis, inflammation, sinusoidal changes, tubular integrity, and myocardial fibre organisation. All samples were documented with unique identifiers to ensure full traceability and reproducibility.

13. Statistical analysis

All quantitative data were expressed as mean ± standard deviation (SD). Statistical analyses were performed using GraphPad Prism (GraphPad Software, San Diego, CA, USA). For the acute oral toxicity study, comparisons among the three groups (vehicle control, 2000 mg/kg, and 5000 mg/kg) were conducted using one-way ANOVA followed by Tukey's honestly significant difference test when the overall F-test was significant ($p < 0.05$). Body weight changes over the 14-day observation period within each group were analysed using repeated-measures ANOVA. A two-tailed p-value < 0.05 was considered statistically significant. Levels of significance were denoted as $*p < 0.05$, $**p < 0.01$, $***p < 0.001$, and $****p < 0.0001$ versus the vehicle control group.

RESULTS

1. FT-IR chromatogram of hot aqueous extract of date palm seed

The infrared (IR) spectrum of the hot aqueous extract of date palm seed (Fig. 1 and Table 1), analysed over a wavenumber range of 3500 to 1000 cm^{-1}, reveals a rich profile of water-soluble constituents. A broad, intense absorption at 3322.2 cm^{-1} (peak area 58.378) indicates O-H stretching from water, carbohydrates, and proteins, reflecting the polar nature of the extract. C-H stretching bands at 2856.1 cm^{-1} (Transmittance 81.893) and 2924.1 cm^{-1} (Transmittance 78.436), along with a C=O stretch at 1742.5 cm^{-1} (Transmittance 83.301), suggest minor contributions from residual lipids or degraded esters. An unusual C≡C stretch at 2146.0 cm^{-1} (Transmittance 84.433) may indicate a contaminant or artefact, requiring further investigation. Peaks at 1610.2 cm^{-1} (Transmittance 88.235) and 1522.6 cm^{-1} (Transmittance 82.061) are attributed to C=C stretching or N-H bending from phenolics, alkaloids or proteins, while C-H bending at 1438.6 cm^{-1} (Transmittance 77.086) and C-O stretching at 1244.9 cm^{-1} (Transmittance 77.741-124.1-

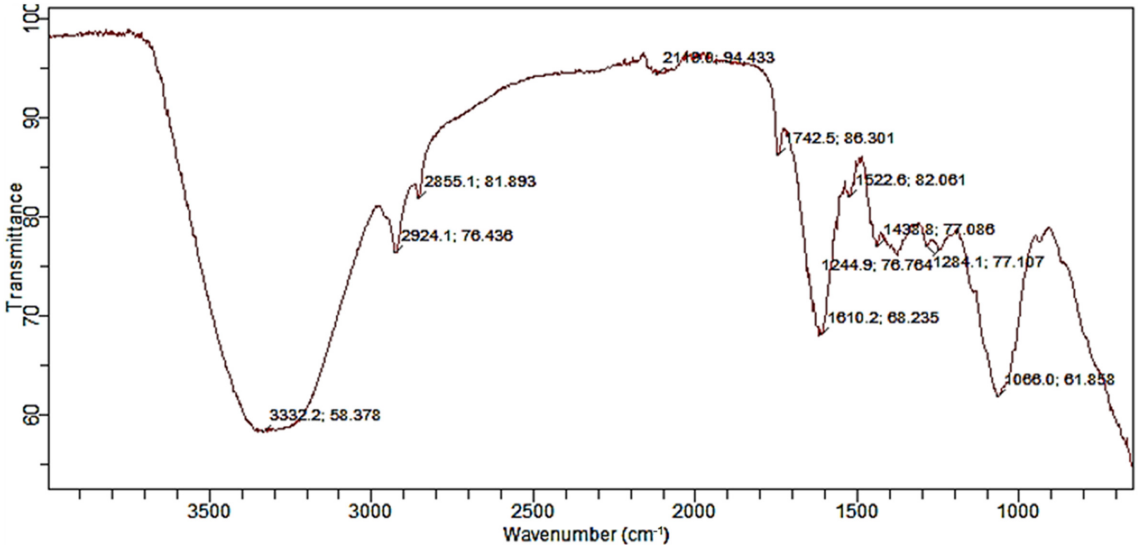


Fig. 1. FT-IR Chromatogram of hot aqueous extract of date palm seed.

Table 1. FT-IR Transmittance, wavenumbers and functional groups of hot aqueous extract of date palm seed.

S/N	Wave numbers (cm^{-1})	Transmittance (%)	Functional groups
1	3322.2	58.378	O–H stretching (water, carbohydrates, or proteins)
2	2924.1	78.436	C–H stretching (residual lipids or carbohydrates)
3	2856.1	81.893	C–H stretching (residual lipids or carbohydrates)
4	2146.1	84.433	C≡C stretching (possible contaminants or artefacts)
5	2146.0	83.301	C=O stretching (possible degraded lipids or esters)
6	1742.5	82.061	N–H bending or C=C stretching (proteins, phenolics or alkaloids)
7	1610.2	88.235	C=C stretching (aromatic rings or phenolics)
8	1522.6	77.086	C–H bending (carbohydrates or proteins)
9	1438.6	77.741 – 124.1 – 77.107	C–O stretching (carbohydrates or polysaccharides)
10	1066.0	61.838	C–O stretching (carbohydrates or esters)

77.107) and 1066.0 cm^{-1} (Transmittance 61.838) confirm a dominant carbohydrate presence, likely polysaccharides.

2. GC–MS chromatogram of hot aqueous extract of date palm seed

The GC–MS chromatogram of the hot aqueous extract of *Phoenix dactylifera* seeds (Fig. 2, Table 2) revealed a diverse profile of volatile and semi-volatile compounds over a retention time range of approximately 6 to 32 min. The most abundant compound was methyl (Z)-9-octadecenoate (methyl oleate) at 13.4612 min, accounting for 27.7661% of the total peak area (quality score 99). Other prominent constituents included methyl 9,12-octadecadienoate (methyl linoleate) at 13.3819 min (7.5834%, quality 99), (Z)-11-octadecenoic acid (cis-vaccenic acid) at 14.2326 min (8.4111%, quality 98), and methyl (R, Z)-12-hydroxyoctadec-9-enoate (methyl ricinoleate) at 16.0865 min (12.7626%, quality 91). Methyl 14-methylpentadecanoate (methyl isopalmitate) was also notable at 11.381 min (7.2726%, quality 98). Minor components included alkanes such as hexadecane (7.5711 min, 1.2244%, quality 97), eicosane (12.1429 min, 2.2267%, quality 96), and nonadecane (11.0277 min, 0.818%, quality 98), as well as the triterpene squalene (23.5239 min,

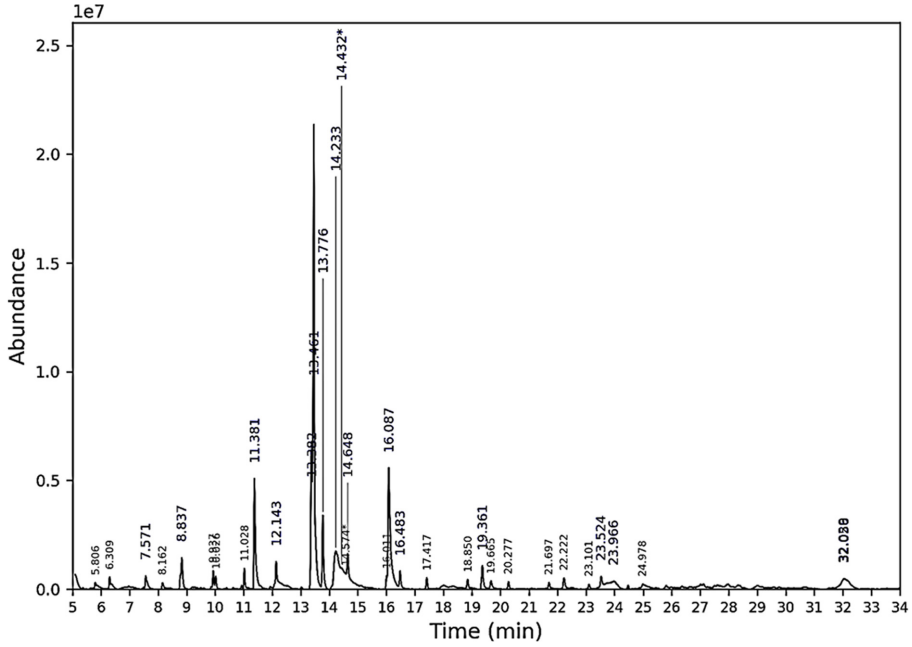


Fig. 2. GC–MS chromatogram of hot aqueous extract of date palm seed.

Table 2. Bioactive compounds present in the hot aqueous extract of date palm seed.

Peak	Name of Compound	Retention time (min)	Peak area (%)	Quality	Molecular Formula
1	Undecane	5.8061	0.4728	74	$C_{11}H_{24}$
2	Pentadecane	6.3086	0.2995	97	$C_{15}H_{32}$
3	Hexadecane	7.5711	1.2244	97	$C_{16}H_{34}$
4	2,6,11-Trimethyldodecane	8.162	0.4247	95	$C_{15}H_{32}$
5	Nonadecane	11.0277	0.818	98	$C_{19}H_{40}$
6	Methyl 14-methylpentadecanoate (methyl isopalmitate)	11.381	7.2726	98	$C_{17}H_{34}O$
7	Eicosane	12.1429	2.2267	96	$C_{20}H_{42}$
8	Methyl 9,12-octadecadienoate (methyl linoleate)	13.3819	7.5834	99	$C_{19}H_{34}O$
9	Methyl (Z)-9-octadecenoate (methyl oleate)	13.4612	27.7661	99	$C_{19}H_{36}O$
10	Methyl stearate	13.7764	4.4052	98	$C_{19}H_{38}O_2$
11	(Z)-11-Octadecenoic acid (cis-vaccenic acid)	14.2326	8.4111	98	$C_{18}H_{34}O_2$
12	(Z)-13-Octadecenoic acid	14.4319	2.5421	98	$C_{18}H_{34}O_2$
13	Oleic acid	14.5736	0.3819	92	$C_{18}H_{34}O_2$
14	(Z)-9-Eicosenoic acid (gondoic acid)	14.6482	3.9002	86	$C_{20}H_{38}O_2$
15	Methyl (R, Z)-12-hydroxyoctadec-9-enoate (methyl ricinoleate)	16.0865	12.7626	91	$C_{19}H_{36}O_2$
16	Methyl 18-methylnonadecanoate	16.4827	1.1325	95	$C_{21}H_{42}O_2$
17	Tetracosane	17.417	0.619	97	$C_{24}H_{50}$
18	Methyl docosanoate (methyl behenate)	19.3614	1.6871	99	$C_{23}H_{46}O_2$
19	Diisooctyl phthalate	19.6652	0.6072	52	$C_{24}H_{38}O_4$
20	Hexacosane	20.2774	0.4295	95	$C_{26}H_{54}$
21	Methyl tetracosanoate (methyl lignocerate)	22.2222	0.8246	96	$C_{25}H_{50}O_2$
22	Heptacosane	23.1009	0.4015	95	$C_{27}H_{56}$
23	Squalene	23.5239	1.3721	64	$C_{30}H_{50}$
24	1-Nonadecene	23.9659	3.2044	86	$C_{19}H_{38}$
25	1-Acetyl-19,21-epoxy-15,16-dimethoxyaspidospermidin-17-ol	24.9781	0.1509	95	$C_{23}H_{30}N_2O_5$
26	Pentatriacont-17-ene	32.029	1.4012	42	$C_{35}H_{70}$
27	Disparlure ((7R,8S)-7,8-epoxy-2-methyloctadecane)	32.0558	2.0686	76	$C_{19}H_{38}O$

1.3721%, quality 64). Trace amounts of 1-nonadecene (23.9659 min, 3.2044%, quality 86) and an indole alkaloid derivative (1-acetyl-19,21-epoxy-15,16-dimethoxyaspidospermidin-17-ol) at 24.9781 min (0.1509%, quality 95) were also detected.

3. Molecular docking

Molecular docking simulations were conducted to evaluate the binding affinities and interaction profiles of seven major bioactive compounds identified from the GC–MS analysis of the hot aqueous extract of roasted date palm (*Phoenix dactylifera*) seeds against human pancreatic α-amylase (EC 3.2.1.1), a key enzyme responsible for hydrolysing dietary starch into absorbable glucose and a validated therapeutic target for post-prandial hyperglycaemia control in type 2 diabetes. Acarbose, a clinically approved α-amylase inhibitor, was used as the positive control for benchmarking binding affinity and interaction modes. The docking protocol, including ligand preparation, receptor structure selection and rationale, grid box parameters, and validation criteria, is described in Section 2.4. Binding affinities (㎉/㏖) and detailed interaction patterns (hydrogen bonding, hydrophobic, polar, and charged interactions) are summarised in Table 3. More negative values indicate stronger predicted binding affinity and more favourable ligand–enzyme interactions.

The binding affinities of the extract-derived ligands ranged from −4.6 ㎉/㏖ (methyl ricinoleate, cis-vaccenic acid, and

Table 3. Binding energies of realistic and promising HAERD ligands from GC-MS results with promising hyperglycaemic activity and Acarbose (positive control) against human pancreatic α−amylase.

Compound name	Pubchem CID	Binding affinity (kcal/mol)	Binding Interaction Pattern between selected Ligands and active site of Human Pancreatic α-Amylase
Methyl Ricinoleate	5354133	−4.6	H-Bonding:None Hydrophobic Interactions:LYS A:457, HIS A:491, ILE A:396, LYS A:35 Polar Interactions:ASP A:456, GLU A:493, SER A:494, ASN A:383, ASN A:399 Charged Interactions:ARG A:392, ARG A:10
Methyl Oleate	5364509	−6.2	H-Bonding:THR A:6 (conventional hydrogen bond) Hydrophobic Interactions:PRO A:332 (alkyl), PHE A:335 Polar Interactions:GLN A:404, SER A:3, THR A:11, ASN A:5 Charged Interactions:ARG A:421, ARG A:398, ASP A:402
Oleic acid	445639	−5	H-Bonding:HIS A:476 (conventional hydrogen bond) Hydrophobic Interactions:ILE A:465, ALA A:483, ILE A:467 (alkyl contacts) Polar Interactions:SER A:454, SER A:480, SER A:478 Charged Interactions:ASP A:451, LYS A:466, ASP A:485
Methyl Linoleate	5284421	-5	H-Bonding:HIS A:491 (conventional hydrogen bond) Hydrophobic Interactions:ILE A:396, LYS A:35, VAL A:400 (alkyl contacts) Polar Interactions:ASN A:393, SER A:494, ASN A:399 Charged Interactions:ASP A:456, ARG A:424, ARG A:392, GLU A:493
(Z)-11-Octadecenoic (cis-vaccenic acid)	5282761	-4.6	H-Bonding:LYS A:457 (conventional hydrogen bond) Hydrophobic Interactions:VAL A:452, ILE A:396, VAL A:400 (alkyl contacts) Polar Interactions:ASN A:399, SER A:494, HIS A:491, ASN A:393 Charged Interactions:ARG A:392, GLU A:493
Methyl 14-methylpentadecanoate	21205	-4.6	H-Bonding:ASN A:399 (conventional hydrogen bond) Hydrophobic Interactions:ILE A:396, LYS A:35, ARG A:10 (alkyl contacts) Polar Interactions:ASN A:393, HIS A:491, SER Charged Interactions:ASP A:456, ARG A:392, GLU A:493, LYS A:457
Squalene	638072	−5.3	H-Bonding:None *(consistent with squalene having no heteroatoms)* Hydrophobic Interactions:ILE A:396, VAL A:452, LYS A:457, HIS A:491 (alkyl/pi-alkyl contacts) Polar Interactions:ASN A:399, ASN A:393 Charged Interactions:ASP A:456, GLU A:493, ARG A:392
Acarbose	9811704	−7.4	H-Bonding:ARG A:421, THR A:6, SER A:289, GLN A:8, PRO A:332, ARG A:252, SER A:3 Polar Interactions:GLN A:404, GLY A:403, THR A:11, GLY A:9, ASN A:5, PHE A:335, TYR A:333, ASP A:290, GLY A:334, PRO A:4, GLN A:7 Charged Interactions:ARG A:398, TYR A:2

methyl 14-methylpentadecanoate) to −6.2 kcal/mol (methyl oleate), with methyl oleate exhibiting the most favourable binding energy among the seven tested phytochemicals. Acarbose (positive control) demonstrated a substantially stronger binding affinity of −7.4 kcal/mol, outperforming all seven extract-derived ligands, consistent with its established role as a potent, clinically validated α-amylase inhibitor. The ligands engaged the enzyme through a combination of hydrophobic (e.g., Ile, Val, Lys, His, Pro, Phe), polar (e.g., Asn, Ser, Gln, Thr, Gly), and charged (e.g., Asp, Glu, Arg) contacts, with conventional hydrogen bonding observed for five of the seven ligands. Notably, none of the seven extract-derived ligands, nor acarbose

itself, formed direct contact with the canonical catalytic triad of human pancreatic α-amylase (Asp197, Glu233, Asp300); instead, all eight ligands converged on a recurring residue cluster distinct from the catalytic centre (including Ile396, Asn393/399, His491, Glu493, Arg392, Asp456, Lys457, and Val400/452 for several of the extract-derived ligands, and a separate residue cluster for acarbose centred on Arg421, Thr6, Ser289, Gln8, Pro332, Arg252, and Ser3). The acarbose pose additionally showed two unfavourable acceptor–acceptor contacts (Asp402, Arg10), indicating some geometric strain in this docking pose. Comprehensive visualisations of the molecular interactions are presented in Figure 3. Each subfigure consists of three panels:

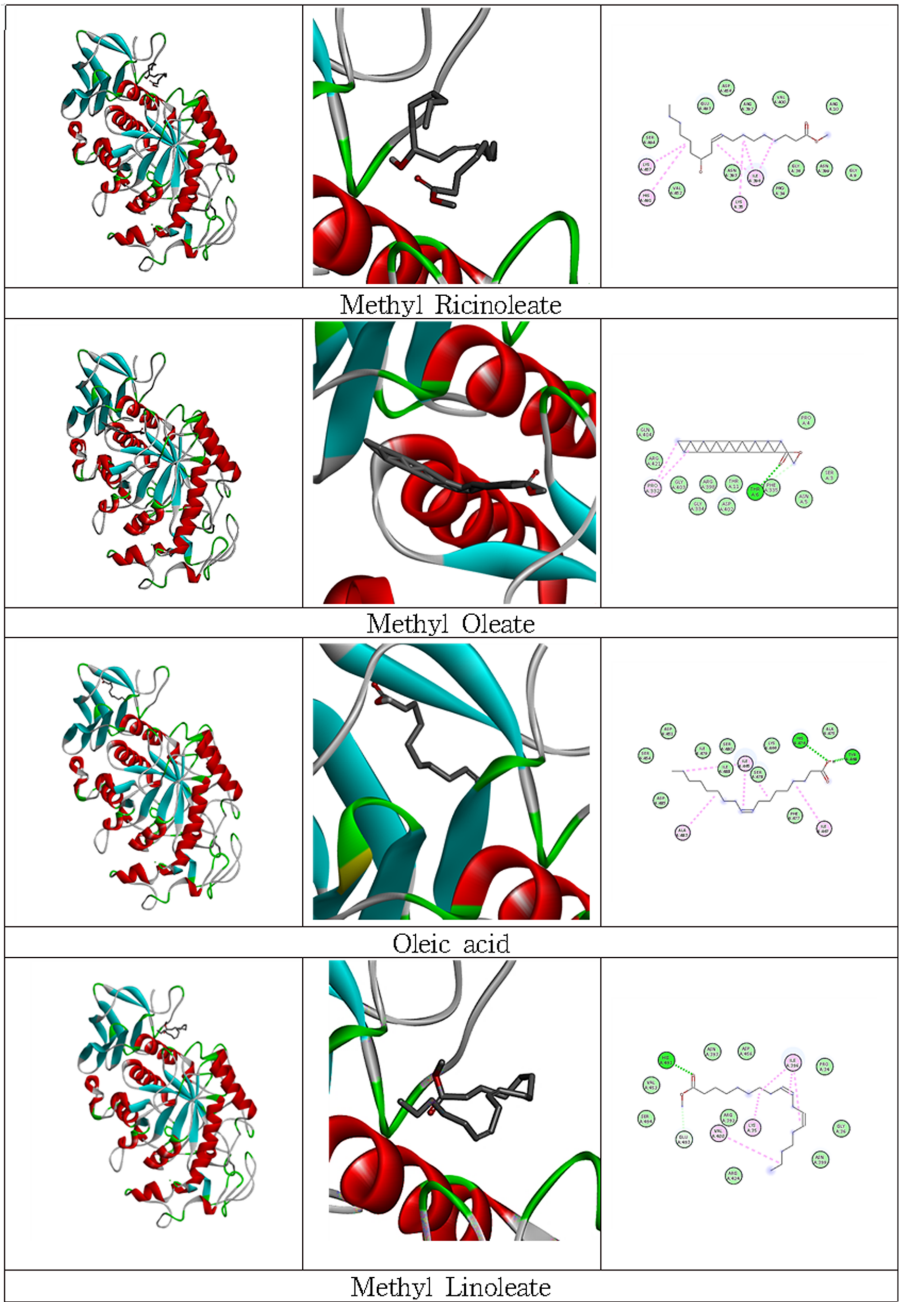


Fig. 3. Illustrations of molecular interactions (left – overall 3D binding pose of the ligand within the protein; middle – close-up 3D view highlighting ligand interactions in the active site; right – 2D interaction diagram showing specific binding contacts) between the realistic and promising ligands for antidiabetic activity and Acarbose (Positive control) against Human Pancreatic amylase.

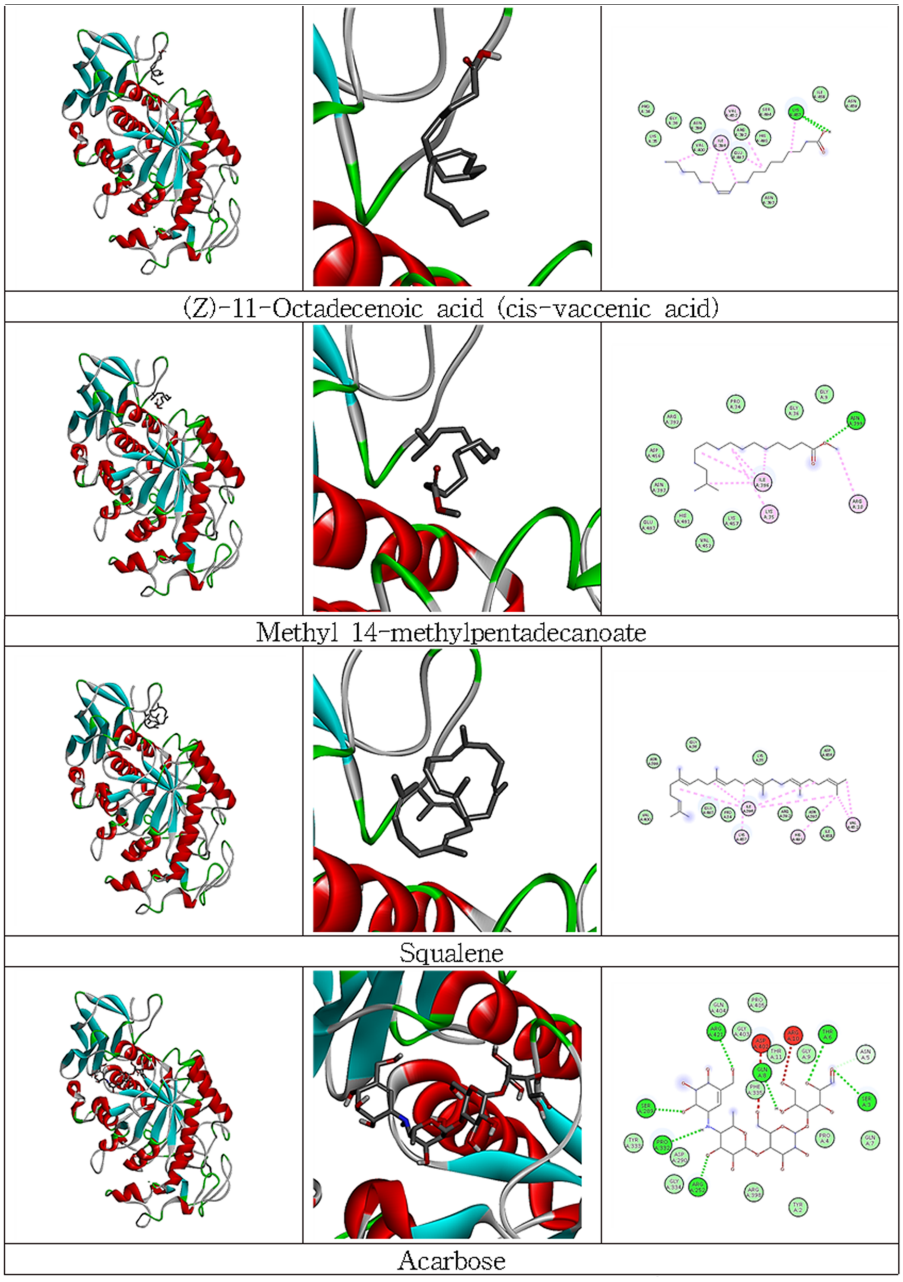


Fig. 3. Continued.

(left) overall 3D binding pose of the ligand within the α-amylase structure; (middle) close-up 3D view highlighting the ligand positioned within the active site; and (right) 2D interaction diagram illustrating specific amino acid residues and interaction types.

I. Methyl (R,Z)-12-hydroxyoctadec-9-enoate (methyl ricinoleate) (PubChem CID 5354133; binding affinity −4.6 kcal/mol) showed no hydrogen bonding but hydrophobic interactions (Lys A:457, His A:491, Ile A:396, Lys A:35), polar interactions (Asp A:456, Glu A:493, Ser A:494, Asn A:383, Asn A:399), and charged interactions (Arg A:392, Arg A:10).

II. Methyl (Z)-9-octadecenoate (methyl oleate) (PubChem CID 5364509; −6.2 kcal/mol) formed a conventional hydrogen bond with Thr A:6, with hydrophobic interactions (Pro A:332, Phe A:335), polar interactions (Gln A:404, Ser

A:3, Thr A:11, Asn A:5), and charged interactions (Arg A:421, Arg A:398, Asp A:402).

III. (Z)-9-Octadecenoic acid (oleic acid) (PubChem CID 445639; −5.0 kcal/mol) formed a conventional hydrogen bond with His A:476, with hydrophobic interactions (Ile A:465, Ala A:483, Ile A:467), polar interactions (Ser A:454, Ser A:480, Ser A:478), and charged interactions (Asp A:451, Lys A:466, Asp A:485).

IV. Methyl 9,12-octadecadienoate (methyl linoleate) (PubChem CID 5284421; −5.0 kcal/mol) formed a conventional hydrogen bond with His A:491, with hydrophobic interactions (Ile A:396, Lys A:35, Val A:400), polar interactions (Asn A:393, Ser A:494, Asn A:399), and charged interactions (Asp A:456, Arg A:424, Arg A:392, Glu A:493).

V. (Z)-11-Octadecenoic acid (cis-vaccenic acid) (PubChem CID 5282761; −4.6 kcal/mol) formed a conventional hydrogen bond with Lys A:457, with hydrophobic interactions (Val A:452, Ile A:396, Val A:400), polar interactions (Asn A:399, Ser A:494, His A:491, Asn A:393), and charged interactions (Arg A:392, Glu A:493).

VI. Methyl 14-methylpentadecanoate (methyl isopalmitate) (PubChem CID 21205; −4.6 kcal/mol) formed a conventional hydrogen bond with Asn A:399, with hydrophobic interactions (Ile A:396, Lys A:35, Arg A:10), polar interactions (Asn A:393, His A:491), and charged interactions (Asp A:456, Arg A:392, Glu A:493, Lys A:457).

VII. (6E,10E,14E,18E)-2,6,10,15,19,23-Hexamethyltetracosa-2,6,10,14,18,22-hexaene (squalene) (PubChem CID 638072; −5.3 kcal/mol) showed no hydrogen bonding, consistent with the absence of heteroatoms in its structure, but hydrophobic interactions (Ile A:396, Val A:452, Lys A:457, His A:491), polar interactions (Asn A:399, Asn A:393), and charged interactions (Asp A:456, Glu A:493, Arg A:392).

4. ADME / Toxicity profile prediction

The predicted pharmacokinetic (ADME) and toxicity profiles

Table 4. Predicted Pharmacokinetic (ADME) and Toxicity Profile of promising HAERD ligands from GC–MS results.

Compound Name	Lipinski violations (SwissADME)	GI Absorption (pkCSM)	BBB Permeability (pkCSM)	CYP450 Inhibition (SwissADME)	Hepatotoxicity (pkCSM)	AMES Mutagenicity (pkCSM)	Oral Toxicity LD_{50} (mol/kg) (pkCSM)
Acarbose	No; 3 violations: MW>500, N or O>10, NH or OH>5	0%	–1.841LogBB	Non-Inhibition	No	No	2.673
Squalene	Yes; 1 violation: MLOGP>4.15	89.002%	0.965LogBB	Non-Inhibition	No	No	1.893
Methyl 14-methylpentadecanoate	Yes; 1 violation: MLOGP>4.15	92.48%	0.748LogBB	Yes (CYP1A2 inhibitor)	No	No	1.606
(Z)-11-Octadecenoic acid	Yes; 1 violation: MLOGP>4.15	91.823%	–0.168LogBB	Yes (CYP1A2 inhibitor, CYP2C9 inhibitor)	No	No	1.417
Methyl Linoleate	Yes; 1 violation: MLOGP>4.15	92.66%	0.767LogBB	Yes (CYP1A2 inhibitor, CYP2C9 inhibitor)	No	No	1.617
Oleic acid	Yes; 1 violation: MLOGP>4.15	91.823%	–0.168LogBB	Yes (CYP1A2 inhibitor, CYP2C9 inhibitor)	No	No	1.417
Methyl Oleate	Yes; 1 violation: MLOGP>4.15	92.154%	0.777LogBB	Yes (CYP1A2 inhibitor)	No	No	1.637
Methyl Ricinoleate	Yes; 0 violations	90.69%	0.101LogBB	Yes (CYP1A2 inhibitor, CYP2C9 inhibitor, CYP3A4 inhibitor).	No	No	1.581

of the promising HAERD ligands identified from GC-MS analysis were evaluated using SwissADME and pkCSM, and the results are presented in Table 4. Acarbose showed three Lipinski rule violations (MW > 500, N or O > 10, and NH or OH > 5). Squalene, methyl 14-methylpentadecanoate, (Z)-11-octadecenoic acid, methyl linoleate, oleic acid, and methyl oleate each exhibited one Lipinski violation (MLOGP > 4.15). Methyl ricinoleate showed no Lipinski violations. Predicted gastrointestinal (GI) absorption was 0% for acarbose. The HAERD compounds displayed GI absorption values ranging from 89.002% (squalene) to 92.66% (methyl linoleate). Blood–brain barrier (BBB) permeability (LogBB) values were −1.841 for acarbose, 0.965 for squalene, 0.748 for methyl 14-methylpentadecanoate, −0.168 for both (Z)-11-octadecenoic acid and oleic acid, 0.767 for methyl linoleate, 0.777 for methyl oleate, and 0.101 for methyl ricinoleate. Regarding CYP450 inhibition, acarbose and squalene were predicted as non-inhibitors. Methyl 14-methylpentadecanoate and methyl oleate were predicted to inhibit CYP1A2. (Z)-11-Octadecenoic acid, methyl linoleate, and oleic acid were predicted to inhibit both CYP1A2 and CYP2C9. Methyl ricinoleate was predicted to inhibit CYP1A2, CYP2C9, and CYP3A4. None of the compounds were predicted to be hepatotoxic or AMES mutagenic. Predicted oral acute toxicity (LD_{50}) values were 2.673 mol/kg for acarbose, 1.893 mol/kg for squalene, 1.606 mol/kg for methyl 14-methylpentadecanoate, 1.417 mol/kg for both (Z)-11-octadecenoic acid and oleic acid, 1.617 mol/kg for methyl linoleate, 1.637 mol/kg for methyl oleate, and 1.581 mol/kg for methyl ricinoleate.

4. Acute toxicity study of the hot aqueous extract of date palm seeds (One-time oral dose toxicity investigation)

The acute oral toxicity of the hot aqueous extract of date palm (*Phoenix dactylifera*) seeds was evaluated in Wistar rats following the OECD Guideline 423 (Acute Toxic Class Method). Animals received a single oral dose of 2000 or 5000 ㎎/㎏ body weight (b.wt.) and were observed for 14 days. Throughout the observation period, no treatment-related mortality or clinical signs of toxicity—including changes in behaviour, locomotion, respiration, posture, or general appearance—were recorded in any treatment group. All extract-treated rats remained clinically normal and comparable to the vehicle control group administered distilled water. Body weight was monitored weekly for two weeks following dosing (Table 5). Rats in all groups exhibited progressive and steady weight gain over the study period. One-way ANOVA revealed no statistically significant differences in body weight within each group across the observation weeks ($p > 0.05$), indicating that acute exposure to the extract, even at 5000 ㎎/㎏ b.wt., did not adversely affect growth performance or general physiological status.

Despite the absence of overt toxicity, histopathological evaluation of the liver, kidney, and heart revealed dose-dependent subclinical tissue alterations (Fig. 4). Control animals displayed normal histological architecture across all organs examined. Liver sections showed well-organised hepatic lobules with prominent central veins, radiating cords of hepatocytes, intact sinusoids, and uniform nuclei. Kidney sections exhibited intact renal corpuscles with well-defined glomeruli and Bowman's spaces, alongside preserved proximal and distal tubules. Cardiac sections revealed regularly aligned myocardial fibres with uniform interfibrillar spaces and distinct nuclei. In rats administered 2000 ㎎/㎏ b.wt., mild histopathological changes were observed. The liver showed slight sinusoidal dilation and hepatocyte swelling with minor central vein congestion. Kidney sections exhibited focal distortion of renal corpuscles with mild tubular dilation, while heart sections demonstrated subtle myocardial fibre disarray accompanied by moderate widening of interfibrillar spaces. These changes were limited and did not substantially disrupt overall tissue architecture. At the 5000 ㎎/㎏ b.wt. dose, histopathological alterations were more pronounced and widespread. Liver sections revealed marked disruption of hepatic lobular organisation, hepatocyte cord disarray, sinusoidal congestion, and nuclear pleomorphism. Kidney sections showed extensive tubular degeneration, depletion of glomerular tufts, and distortion of renal corpuscles. Cardiac

Table 5. Body weight values (g) of Wistar rats orally administered with hot aqueous extract of date palm seeds in a single-dose study (N = 3 per group). Data are expressed as mean ± SD (N = 3). Values within the same treatment group (column) with different superscripts (a, b, c) are significantly different across weeks (one-way ANOVA followed by Tukey's post hoc test, $p < 0.05$).

Group	Week 1	Week 2	Week 3	*F* value	P value
Control	111.33 ± 16.29[a]	124.00 ± 20.00[a]	142.67 ± 25.32[a]	1.71	0.258
2000 ㎎/㎏ b.wt	146.67 ± 5.77[a]	163.33 ± 15.28[a]	160.00 ± 20.00[a]	1.05	0.406
5000 ㎎/㎏ b.wt	150.00 ± 10.00[a]	176.67 ± 15.28[a]	170.00 ± 24.98[a]	1.81	0.243

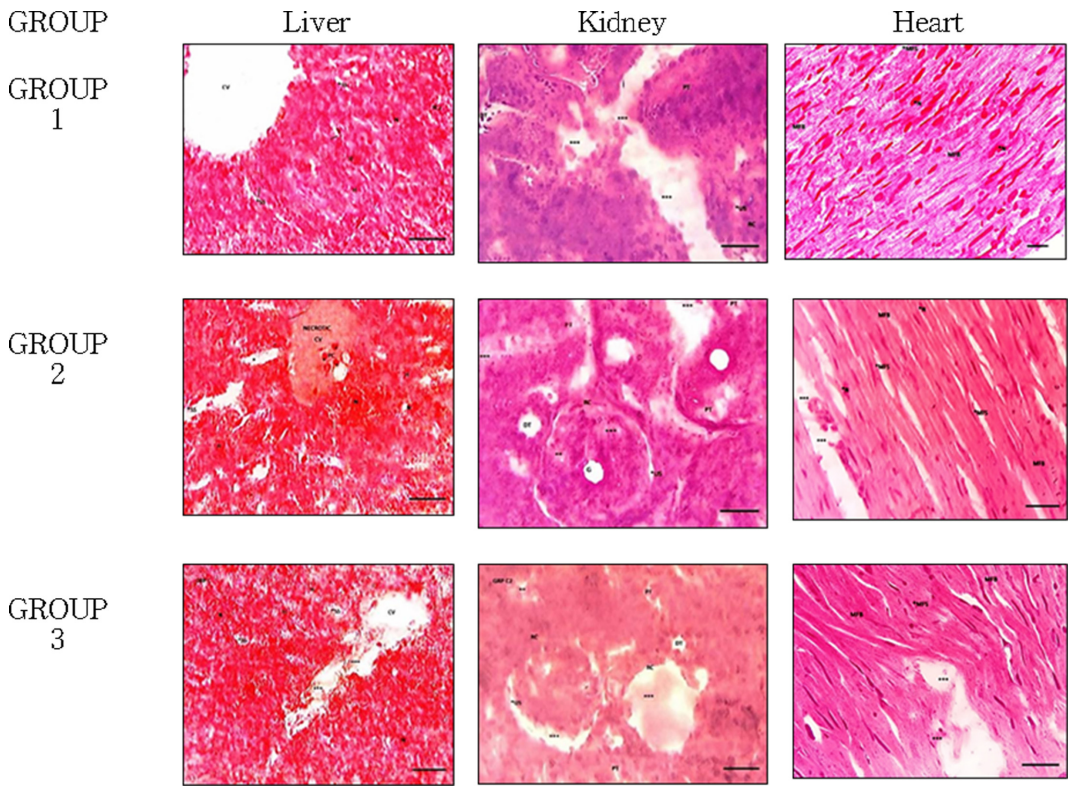


Fig. 4. Histopathological findings in the liver, kidney, and heart of Wistar rats administered a single oral dose of hot aqueous extract of date palm (*Phoenix dactylifera*) seeds at 2000 mg/kg body weight (Group II), 5000 mg/kg body weight (Group III) and those given the vehicle (distilled water) only (Group I). (400 ×). MFB=muscle fibres, XX=lesions, MFS = myofibrilla space, N=nuclei, XXX=distortions, PT=proximal tubules, DT=distal tubules, G = glomerulus, GS=glomerular space, CV=central vein, SS=sinusoids, H=hepatocytes, US=Urinary space, RC=Renal corpuscle.

tissue exhibited pronounced myocardial fibre disorganisation with substantial interfibrillar oedema, indicative of dose-related cardiac injury.

DISCUSSION

The present study provides a comprehensive phytochemical characterisation, in silico mechanistic insight, and safety assessment of the hot water infusion of roasted *Phoenix dactylifera* seeds (HAERD). By linking traditional processing methods with modern analytical and computational approaches, the results strengthen the scientific basis for its ethnomedicinal use in the management of type 2 diabetes and associated metabolic disorders, while highlighting its potential as a sustainable nutraceutical derived from agricultural waste.

FT-IR spectral features were tentatively consistent with a polar, carbohydrate-rich matrix potentially containing polysaccharides, proteins, and phenolic/aromatic-type compounds, while GC–MS confirmed unsaturated fatty acid methyl esters as the dominant identified constituents, with methyl oleate as the most abundant (27.77%); notably, no phenolic compounds were among the 27 constituents identified by GC–MS. These results are consistent with previous phytochemical studies on date palm seeds, which have consistently reported high levels of oleic acid derivatives and phenolic compounds in both seed oils and aqueous extracts (Alkhoori *et al*., 2022; Besbes *et al*., 2004; Al-Farsi and Lee, 2008b). The elevated methyl oleate content observed here (27.77%) is higher than values typically reported for many Middle Eastern cultivars (often 15–22% in seed oils), suggesting possible varietal, geographical, or processing-related differences that favour greater accumulation or extractability of this bioactive ester in West African date palms (Besbes *et al*., 2004; Sui *et al*., 2019). Roasting plays a critical role in this profile: heat not only breaks down the rigid cell wall matrix, facilitating the release of bound lipids and potential phenolic-type compounds into the aqueous phase, but also promotes mild esterification and Maillard-type reactions that enhance the formation and extractability of fatty acid

methyl esters (Ismail *et al*., 2025; Sui *et al*., 2019).

The most significant finding was that acarbose, the positive control, showed the strongest predicted binding affinity of all eight ligands tested (−7.4 ㎉/㏖), outperforming the best extract-derived ligand, methyl oleate (−6.2 ㎉/㏖), by 1.2 ㎉/㏖. Notably, methyl oleate's binding footprint substantially overlaps with acarbose's: methyl oleate formed a conventional hydrogen bond with Thr6 and additional contacts with Pro332, Phe335, Gln404, Ser3, Thr11, Asn5, Arg421, Arg398, and Asp402 — nearly all of which also appear among acarbose's own contact residues (Arg421, Thr6, Ser289, Gln8, Pro332, Arg252, Ser3, among others). This suggests methyl oleate occupies a sub-region of the same binding groove used by acarbose, which may plausibly explain its comparatively modest but non-trivial affinity: acarbose, as a larger pseudo-tetrasaccharide, forms a substantially more extensive hydrogen-bonding network (seven conventional hydrogen bonds spanning multiple subsites) than methyl oleate's single hydrogen bond, consistent with its markedly stronger predicted affinity. Notably, neither methyl oleate nor acarbose — nor any of the other six extract-derived ligands — formed direct contact with the canonical catalytic triad of human pancreatic α-amylase (Asp197, Glu233, Asp300) in these docking poses; all eight ligands instead converged on residue clusters located elsewhere within the broader substrate-binding cleft. The precise inhibitory mechanism of methyl oleate and the other extract-derived compounds therefore remains a hypothesis that requires experimental confirmation, such as enzyme kinetics studies capable of distinguishing competitive from non-competitive or allosteric inhibition modes. The conformational flexibility of the long-chain fatty acid ester likely contributes to its binding within this subsite. Although methyl esters may also act as prodrugs that undergo *in vivo* hydrolysis by esterases to release free oleic acid (Lerin *et al*., 2024; Dong *et al*., 2025), methyl oleate itself is predicted, based on the docking model, to bind human pancreatic α-amylase directly. These in silico results fall within the broader literature range reported for plant-derived natural α-amylase inhibitors, which frequently report binding affinities in the −4.5 to −9.0 ㎉/㏖ range (Rangel-Galván *et al*., 2024; Singh *et al*., 2025).

The in silico ADME and toxicity profiling of the HAERD-derived ligands provides further insight into their potential as orally bioavailable candidates relative to the reference α-amylase inhibitor acarbose. Acarbose exhibited three violations of Lipinski's rule of five (molecular weight > 500 Da, number of hydrogen-bond acceptors > 10, and number of hydrogen-bond donors > 5; Lipinski *et al*., 1997). This is consistent with its well-documented poor systemic absorption (less than 2% of an oral dose is absorbed as active drug), which is therapeutically desirable for a locally acting intestinal agent but limits its utility when systemic exposure is required (McIver *et al*., 2024). In contrast, most of the HAERD-derived compounds showed only a single violation (MLOGP > 4.15), while methyl ricinoleate fully complied with Lipinski's criteria (zero violations); compliance with, or minimal deviation from, Lipinski's guidelines is generally associated with improved oral bioavailability (Lipinski *et al*., 1997). Predicted gastrointestinal absorption further highlighted this contrast: acarbose was predicted to have essentially no GI absorption (0%), whereas the HAERD-derived compounds displayed high predicted absorption (89–93%), consistent with the physicochemical properties expected of fatty-acid derivatives and squalene. Blood–brain barrier (BBB) permeability predictions varied across the series: positive LogBB values for squalene, methyl 14-methylpentadecanoate, methyl linoleate, and methyl oleate suggest potential CNS penetration (LogBB > 0.3 is generally considered indicative of ready BBB crossing; Pires *et al*., 2015), whereas (Z)-11-octadecenoic acid, oleic acid, and methyl ricinoleate showed low or negative LogBB values indicating more limited CNS exposure. Metabolic liability assessment showed acarbose and squalene as predicted non-inhibitors of the major CYP450 isoforms, while several fatty-acid methyl esters and free fatty acids were flagged as inhibitors of CYP1A2 and, in some cases, CYP2C9 or CYP3A4; although CYP inhibition does not preclude further development, it signals a potential for drug–drug interactions warranting experimental verification. Importantly, none of the eight compounds were predicted to be hepatotoxic or mutagenic in the AMES assay. Predicted acute oral toxicity (LD_{50}) values for the HAERD-derived ligands (1.417–1.893 mol/kg) were lower than that of acarbose (2.673 mol/kg) but remained within a range considered relatively safe by the computational models employed. Overall, this computational ADME/toxicity profile suggests that several HAERD-derived ligands — particularly methyl ricinoleate (full Lipinski compliance, high GI absorption) and squalene (high absorption, absence of predicted CYP450 inhibition) — display more favourable predicted oral bioavailability and drug-likeness characteristics than acarbose, while maintaining an acceptable predicted safety margin. These in silico findings support prioritising these candidates for subsequent experimental

pharmacokinetic, metabolic, and *in vivo* efficacy studies, alongside the *in vitro* enzyme-inhibition validation already noted as essential above.

Beyond its predicted inhibitory potential, the safety profile of HAERD was evaluated to determine its suitability for long-term consumption. No mortality or overt clinical signs of toxicity were observed up to the limit dose of 5000 ㎎/㎏ body weight (estimated LD_{50} > 5000 ㎎/㎏, GHS Category 5), in accordance with OECD Guideline 423. Body weight gain remained progressive and comparable to controls ($p > 0.05$), indicating that acute exposure did not impair general physiological status. However, histopathological examination revealed dose-dependent subclinical alterations. At 2000 ㎎/㎏, changes were mild: sinusoidal dilation and hepatocyte swelling in the liver, focal tubular dilation in the kidney, and subtle myocardial fibre disarray. At the limit dose of 5000 ㎎/㎏, these alterations were substantially more severe: the liver showed marked disruption of hepatic lobular organisation, hepatocyte cord disarray, sinusoidal congestion, and nuclear pleomorphism; the kidney showed extensive tubular degeneration, depletion of glomerular tufts, and distortion of renal corpuscles; and cardiac tissue showed pronounced myocardial fibre disorganisation with substantial interfibrillar oedema, findings consistent with dose-related cardiac injury. No mortality or overt clinical signs accompanied these changes, but the extract cannot be considered free of target-organ effects at supra-therapeutic doses, and the acute safety margin should be interpreted with corresponding caution rather than characterised as uniformly favourable. These findings are consistent with previous acute toxicity studies on aqueous date seed extracts, which also reported LD_{50} values exceeding 2000–5000 ㎎/㎏ with no overt clinical toxicity but occasional mild histopathological changes at high doses (Fakhri *et al*., 2018; Alqarni et al., 2019). Similar safety profiles have been documented for other Nigerian medicinal plants used in metabolic disorders, such as *Vernonia amygdalina* and *Gongronema latifolium*, which showed LD_{50} values > 5000 ㎎/㎏ with only mild organ changes at supra-therapeutic doses yet demonstrated strong antioxidant and hepatoprotective effects in diet-induced models (Ugochukwu *et al*., 2003; Egedigwe *et al*., 2016). The absence of histopathological changes at doses in the traditional-use range (200–500 ㎎/㎏) — well below both the 2000 ㎎/㎏ dose at which mild changes first appeared and the 5000 ㎎/㎏ limit dose — offers some reassurance for use at traditionally consumed levels, although this lower dose range was not directly tested in the present study and should be confirmed by a dedicated sub-chronic toxicity study.

The antioxidant contribution anticipated from the FT-IR-suggested phenolic/aromatic functional groups and the unsaturated fatty acid derivatives identified by GC–MS may help mitigate oxidative stress, a key factor in hyperglycaemia and associated complications; however, phenolic content was not quantitatively determined in this study, and its antioxidant contribution remains inferential pending a confirmatory assay (e.g., Folin–Ciocalteu total phenolic content) and direct antioxidant testing. These constituents, well-documented for their free radical scavenging capacity in date palm seed preparations, provide an additional mechanistic dimension to the extract's potential value (Rock *et al*., 2009; Mia *et al*., 2020; Alkhoori *et al*., 2022;). This antioxidant potential complements the α-amylase-binding potential of methyl oleate predicted by the molecular docking studies, suggesting that the crude extract may exert multi-target effects relevant to metabolic health, pending experimental confirmation of the enzyme-inhibition component. Synergistic interactions among the identified fatty acid methyl esters (FAMEs), FT-IR-suggested phenolic-type compounds, and polysaccharides could further enhance the overall bioactivity of HAERD beyond single-enzyme inhibition (Ganesan and Xu, 2019; de Paulo Farias, 2021).

Strengths of this study include the integration of traditional roasting and hot water infusion with modern analytical (FT-IR, GC–MS) and computational techniques, offering both chemical fingerprinting and computational mechanistic insight into potential α-amylase inhibition. Limitations include the in silico nature of the docking (static model without molecular dynamics), the use of male rats only in the toxicity assessment, small sample size, and the lack of isolated compound testing or *in vitro* enzyme kinetics. Critically, the reported binding affinities and inhibitory potential of methyl oleate and other extract constituents are computational predictions only; no *in vitro* or *in vivo* enzyme-inhibition assay has yet been performed to experimentally validate these docking results, and no claim of proven α-amylase inhibitory activity is made in this study. Furthermore, the docking results characterise the predicted activity of seven individual constituents in isolation; they do not capture potential synergistic, additive, or antagonistic interactions among the many co-occurring compounds in the crude extract, nor do they account for compounds present in the extract but not identified or tested (e.g., non-volatile or polar constituents not amenable to GC–MS). Extrapolating

from these seven tested constituents to the bioactivity of the whole HAERD extract therefore remains an inference that requires direct confirmation using the intact extract itself. These constraints are consistent with preliminary safety screening aligned with the 3Rs principles.

Collectively, the results support the traditional use of roasted date palm seed infusion and its potential development as a low-cost, multi-target nutraceutical. By valorising date palm seed agro-waste — an abundant and underutilised resource in Nigeria and other date-producing regions — this approach offers both economic and environmental benefits while contributing to sustainable diabetes management strategies. Experimental validation via *in vitro* α-amylase inhibition assays (e.g., chromogenic or reducing-sugar-based methods using purified enzyme and isolated methyl oleate) is an essential next step before the predicted inhibitory activity can be considered established. Future work should also include molecular dynamics simulations, bioactivity-guided fractionation, chronic toxicity studies in both sexes, and ultimately clinical trials to confirm efficacy and safety in humans.

In conclusion, the hot water infusion of roasted *Phoenix dactylifera* seeds (HAERD) is characterised by a rich profile of water-soluble bioactives, with methyl oleate emerging as the predominant constituent. Molecular docking studies indicated that methyl oleate exhibits a moderate predicted binding affinity to human pancreatic α-amylase (−6.2 ㎉/㏖), within a binding groove overlapping that of the reference inhibitor acarbose, though acarbose itself showed the strongest predicted affinity of all eight ligands tested (−7.4 ㎉/㏖). This in silico finding highlights the potential of HAERD as a natural modulator of carbohydrate digestion, pending experimental validation. Acute oral toxicity evaluation according to OECD Guideline 423 showed no mortality or overt clinical signs of toxicity up to 5000 ㎎/㎏ (estimated LD_{50} > 5000 ㎎/㎏), but histopathological evaluation revealed dose-dependent hepatic, renal, and cardiac alterations that became marked at the limit dose — including hepatocellular disorganisation with sinusoidal congestion and nuclear pleomorphism, renal tubular degeneration with glomerular tuft depletion, and myocardial fibre disorganisation with interfibrillar oedema consistent with dose-related cardiac injury. These findings indicate that HAERD is not free of target-organ effects at supra-therapeutic doses, and its overall safety margin should be interpreted with appropriate caution pending sub-chronic and dose-range toxicity studies. Collectively, these results position the hot aqueous extract of roasted date palm seeds as a promising, low-cost candidate derived from agricultural waste for further development as a nutraceutical or adjunct therapeutic agent in the management of hyperglycaemia. Future studies should prioritise *in vitro* enzyme inhibition assays to experimentally validate the docking-predicted α-amylase inhibitory potential, alongside bioactivity-guided fractionation and chronic toxicity evaluations, to advance its translational potential.

ACKNOWLEDGMENT

We thank the Imo State University Owerri, Department of Biochemistry staff for their assistance and access to research facilities.

REFERENCES

Alfaleh AA and Sindi HA. (2024). Systematic study on date palm seeds(*Phoenix dactylifera* L.) extraction optimisation using natural deep eutectic solvents and ultrasound technique. Scientific Reports. 14:16622.

Al-Farsi MA and Lee CY. (2008a). Nutritional and functional properties of dates: A review. Critical Reviews in Food Science and Nutrition. 48:877-887.

Al-Farsi MA and Lee CY. (2008b). Optimization of phenolics and dietary fibre extraction from date seeds. Food Chemistry. 108:977-985.

Al Juhaimi F, Özcan MM, Ghafoor K and Babiker EE. (2018). The effect of microwave roasting on bioactive compounds, antioxidant activity and fatty acid composition of apricot kernel and oils. Food Chemistry. 243:414-419.

Alkhoori MA, Kong ASY, Aljaafari MN, Abushelaibi A, Erin Lim SH, Cheng WH, Chong ㎝ and Lai KS. (2022). Biochemical composition and biological activities of date palm(*Phoenix dactylifera* L.) seeds: A review. Biomolecules. 12:1626. https://www.mdpi.com/2218-273X/12/11/1626 (cited by 2026 Sep 28).

Alqarni MMM, Osman MA, Al-Tamimi DS, Gassem MA, Al-Khalifa AS, Al-Juhaimi F and Mohamed Ahmed IA. (2019). Antioxidant and antihyperlipidemic effects of Ajwa date(*Phoenix dactylifera* L.) extracts in rats fed a cholesterol-rich diet. Journal of Food Biochemistry. 43:e12933.

Berman HM, Westbrook J, Feng Z, Gilliland G, Bhat TN, Weissig H, Shindyalov IN and Bourne PE. (2000). The Protein Data Bank. Nucleic Acids Research. 28:235-242.

Besbes S, Blecker C, Deroanne C, Bahloul N, Lognay G, Drira NE and Attia H. (2004). Date seed oil: Phenolic, tocopherol and sterol profiles. Journal of Food Lipids. 11:251-265.

Brayer GD, Luo Y and Withers SG. (1995). The structure of human pancreatic α-amylase at 1.8 Å resolution and comparisons with related enzymes. Protein Science. 4:1730-1742.

Daina A, Michielin O and Zoete V. (2017). SwissADME: A free web tool to evaluate pharmacokinetics, drug-likeness and medicinal chemistry friendliness of small molecules. Scientific

Reports. 7:42717.

de Paulo Farias D, de Araújo FF, Neri-Numa IA and Pastore GM. (2021). Antidiabetic potential of dietary polyphenols: A mechanistic review. Food Research International. 145:110383.

Djaoudene O, Rodríguez-Solana R and Romano A. (2026). Valorization of date palm(*Phoenix dactylifera* L.) fruits and by-products as high-value sustainable products: A comprehensive review on bioactive composition, health benefits, and industrial applications. Molecules. 31:1194. https://www.mdpi.com/1420-3049/31/7/1194 (cited by 2026 Sep 28).

Dong X, Zhang T, Moreno Sanchez HL, Mans JC, Bae SH and Bian L. (2025). Enhancing oral absorption of an ester prodrug by coating drug crystals with binary lipid systems and evaluating the influence of compositions. Pharmaceutics. 17:1210. https://www.mdpi.com/1999-4923/17/9/1210 (cited by 2026 Sep 28).

Egedigwe CA, Ijeh II, Okafor PN and Ejike CECC. (2016). Aqueous and methanol extracts of *Vernonia amygdalina* leaves exert their anti-obesity effects through the modulation of appetite-regulatory hormones. Pharmaceutical Biology. 54:3232-3236.

Fakhri S, Shokoohinia P, Marami M, Ghiasvand N, Hosseinzadeh L and Shokoohinia Y. (2018). Acute and sub-chronic toxicity evaluation of aqueous extract of *Phoenix dactylifera* seeds in Wistar rats. Journal of Reports in Pharmaceutical Sciences. 7:319-330.

Ganesan K and Xu B. (2019). Anti-diabetic effects and mechanisms of dietary polysaccharides. Molecules. 24:2556. https://www.mdpi.com/1420-3049/24/14/2556 (cited by 2026 Sep 28).

Genitsaridi I, Salpea P, Salim A, Sajjadi SF, Tomic D, James S, Thirunavukkarasu S, Issaka A, Chen L, Basit A, Luk AOY, Ma RCW, Mbanya JC, Ramachandran A, Wild SH, Duncan BB, Boyko EJ and Magliano DJ. (2026). 11th edition of the IDF Diabetes Atlas: Global, regional, and national diabetes prevalence estimates for 2024 and projections for 2050. The Lancet Diabetes & Endocrinology. 14:149-156.

Hasan M and Mohieldein A. (2016). *In vivo* evaluation of anti diabetic, hypolipidemic, antioxidative activities of Saudi date seed extract on streptozotocin induced diabetic rats. Journal of Clinical and Diagnostic Research. 10:FF06-FF12.

International Diabetes Federation. (2025). IDF Diabetes Atlas. 11th ed. International Diabetes Federation. Brussels, Belgium.

Ismail WM, Zayed A, Ramadan NS, Sakna ST and Farag MA. (2025). GC-MS based nutritional and aroma profiling of date palm seeds collected from different Egyptian cultivars for valorization purposes. Scientific Reports. 15:16531.

Khan TJ, Kuerban A, Razvi SS, Mehanna MG, Khan KA, Almulaiky YQ and Faidallah HM. (2018). *In vivo* evaluation of hypolipidemic and antioxidative effect of 'Ajwa'(*Phoenix dactylifera* L.) date seed-extract in high-fat diet-induced hyperlipidemic rat model. Biomedicine & Pharmacotherapy. 107:675-680.

Lerin LA, Botti G, Dalpiaz A, Bianchi A, Ferraro L, Chaibi C, Zappaterra F, Meola D, Giovannini PP and Pavan B. (2024). Characterization and hydrolysis studies of a prodrug obtained as ester conjugate of geraniol and ferulic acid by enzymatic way. International Journal of Molecular Sciences. 25:6263.

Li J, Hussain I, Azam M, Khan MA, Akram MT, Naveed K, Asif M, Anjum N, Zeng J, Zhang J and Liu H. (2023). Hot water treatment improves date drying and maintains phytochemicals and fruit quality characteristics of date palm(*Phoenix dactylifera*). Foods. 12:2405. https://www.mdpi.com/2304-8158/12/12/2405 (cited by 2026 Sep 28).

Lipinski CA, Lombardo F, Dominy BW and Feeney PJ. (1997). Experimental and computational approaches to estimate solubility and permeability in drug discovery and development settings. Advanced Drug Delivery Reviews. 23:3-25.

Maruthur NM, Tseng E, Hutfless S, Wilson LM, Suarez-Cuervo C, Berger Z, Chu Y, Iyoha E, Segal JB and Bolen S. (2016). Diabetes medications as monotherapy or metformin-based combination therapy for type 2 diabetes: A systematic review and meta-analysis. Annals of Internal Medicine. 164: 740-751.

Mia MAT, Mosaib MG, Khalil MI, Islam MA and Gan SH. (2020). Potentials and safety of date palm fruit against diabetes: A critical review. Foods. 9:1557. https://www.mdpi.com/2304-8158/9/11/1557 (cited by 2026 Sep 28).

Morris GM, Huey R, Lindstrom W, Sanner MF, Belew RK, Goodsell DS and Olson AJ. (2009). AutoDock4 and AutoDockTools4: Automated docking with selective receptor flexibility. Journal of Computational Chemistry. 30:2785-2791.

Nahoum V, Roux G, Anton V, Rougé P, Puigserver A, Bischoff H, Henrissat B and Payan F. (2000). Crystal structures of human pancreatic α-amylase in complex with carbohydrate and proteinaceous inhibitors. Biochemical Journal. 346:201-208.

National Institute of Standards and Technology. (2014). NIST/EPA/NIH Mass Spectral Library(NIST 14). NIST Standard Reference Database 1A. National Institute of Standards and Technology. Gaithersburg, Maryland, USA.

National Research Council. (2011). Guide for the care and use of laboratory animals. 8th ed. The National Academies Press. Washington, DC, USA.

Organisation for Economic Co-operation and Development. (2002). Test No. 423: Acute oral toxicity – acute toxic class method. OECD Guidelines for the Testing of Chemicals, Section 4. OECD Publishing. Paris, France. p.1-14.

Percie du Sert N, Hurst V, Ahluwalia A, Alam S, Avey MT, Baker M, Browne WJ, Clark A, Cuthill IC, Dirnagl U, Emerson M, Garner P, Holgate ST, Howells DW, Karp NA, Lazic SE, Lidster K, MacCallum CJ, Macleod M, Pearl EJ, Petersen OH, Rawle F, Reynolds P, Rooney K, Sena ES, Silberberg SD, Steckler T and Würbel H. (2020). The ARRIVE guidelines 2.0: Updated guidelines for reporting animal research. PLOS Biology. 18:e3000410.

Pires DEV, Blundell TL and Ascher DB. (2015). pkCSM: Predicting small-molecule pharmacokinetic and toxicity properties using graph-based signatures. Journal of Medicinal Chemistry. 58:4066-4072.

Rangel-Galván M, Pacheco-Hernández Y, Lozoya-Gloria E and Villa-Ruano N. (2024). Dietary natural products as inhibitors of α-amylase and α-glucosidase: An updated review of ligand-receptor correlations validated by docking studies. Food Bioscience. 62:105456.

Rock W, Rosenblat M, Borochov-Neori H, Volkova N, Judeinstein S, Elias M and Aviram M. (2009). Effects of

date(*Phoenix dactylifera* L., Medjool or Hallawi variety) consumption by healthy subjects on serum glucose and lipid levels and on serum oxidative status: A pilot study. Journal of Agricultural and Food Chemistry. 57:8010-8017.

Silverstein RM, Webster FX, Kiemle DJ and Bryce DL. (2015). Spectrometric identification of organic compounds. 8th ed. John Wiley & Sons. Hoboken, New Jersey, USA.

Singh R, Sindhu J, Singh D and Kumar P. (2025). Key molecular scaffolds in the development of clinically viable α-amylase inhibitors. Future Medicinal Chemistry. 17:347-362.

Sui W, Mu T, Sun H and Yang H. (2019). Effects of different drying methods on nutritional composition, physicochemical and functional properties of sweet potato leaves. Journal of Food Processing and Preservation. 43:e13884.

Suvarna SK, Layton C and Bancroft JD. (eds.). (2019). Bancroft's theory and practice of histological techniques. 8th ed. Elsevier. Oxford, England.

Swaidan A, Azakir B, Neugart S, Kattour N, Sokhn ES, Osaili TM and Darra NE. (2024). Evaluation of the phenolic composition and biological activities of six aqueous date (*Phoenix dactylifera* L.) seed extracts originating from different countries: A comparative analysis. Foods. 13:126. https://www.mdpi.com/2304-8158/13/1/126 (cited by 2026 Sep 28).

Ugochukwu NH, Babady NE, Cobourne M and Gasset SR. (2003). The effect of *Gongronema latifolium* extracts on serum lipid profile and oxidative stress in hepatocytes of diabetic rats. Journal of Biosciences. 28:1-5.

Vayalil PK. (2012). Date fruits(*Phoenix dactylifera* Linn): An emerging medicinal food. Critical Reviews in Food Science and Nutrition. 52:249-271.